Operational Experience with the ELENA Ion Source

Davide Gamba,[1, a)] Davide Aguglia,[1] Bertrand Lefort,[1] Christophe Machado,[1] Fredrik Wenander,[1] and Ralf Gebel[2]

[1)] *CERN European Organization for Nuclear Research, Geneva, Switzerland.*
[2)] *Forschungszentrum Jülich GmbH, IKP-4, 52425, Jülich, Germany.*

[a)] *Corresponding author: davide.gamba@cern.ch*

Abstract. The Extremely Low ENergy Antiproton (ELENA) is a compact ring that was recently installed to complement the antimatter factory at CERN. A local H^-/p source is connected to ELENA for commissioning purposes of the ring and subsequent electrostatic transfer lines toward experiments, allowing to progress with the commissioning phase also in the absence of antiprotons. The ELENA source can produce pulses of H^-, with a length of a few µs and an intensity of approximately 50 µA at 100 keV, to mimic the antiproton pulse at extraction energy. In addition, the source can deliver proton pulses, if need be. After a few years of operation, several observations have been collected that will be presented in this work. Of particular interest is the observation of a fast (about 1 MHz) intra-pulse instability for H^-, which resulted in poor intensity stability of the H^- beam injected into ELENA. Possible ways of stabilising the beam pulse have been found and will also be presented.

INTRODUCTION

The Antimatter Factory at CERN was recently extended with the installation of the ELENA ring [1]. Until now most antimatter experiments by CERN were taking antiproton (pbar) beams directly from the Antiproton Decelerator (AD) [2], which can provide the experiments with approximately 3×10^7 antiprotons per pulse at an energy of 5.3 MeV. For such kinetic energy, the antiproton trapping efficiency at the experiments is poor, typically less than a percent. With the addition of the ELENA ring, the antiproton beam energy is further decelerated to 100 keV, which will allow experiments to increase their trapping efficiency by up to two orders of magnitude.

The ELENA project was approved at CERN in June 2011 and construction began two years later [3]. As AD is only able to provide one antiproton pulse approximately every 110 seconds, the ELENA project foresaw the installation of a local H^- source with a higher repetition rate that would avoid interference with the experimental program of AD, and allow faster progress with the commissioning of the ELENA ring and transfer lines. The H^- source has been specified to deliver a beam that can mimic the antiproton beam at the lowest kinetic energy, i.e. approximately 3×10^7 H^- in a single bunch of about 250 ns length and 1 µm normalised emittance [1], to be directly injected into the ring.

The first circulating H^- beam was observed already in November 2016 [4], even though the ring installation was only completed at the beginning of 2018 with the insertion and commissioning of its electron cooler [5].

The first commissioning with antiproton from AD was completed in 2018 [6], just before the start of the CERN Long Shutdown two (LS2). During the first part of LS2 (2019-2020), the main activity was the installation and

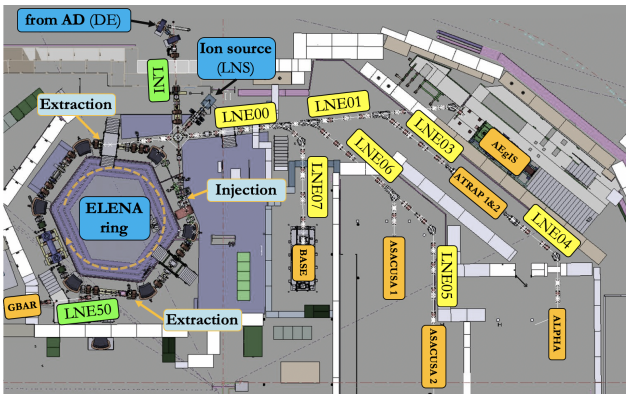

FIGURE 1. Layout of the ELENA hall. The transfer lines names (yellow and green), experiments (orange) and key components (blue) are highlighted.

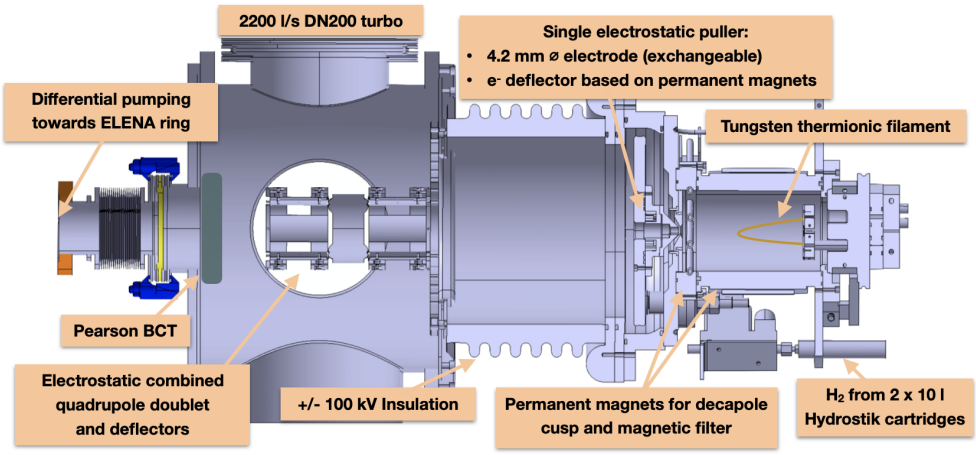

FIGURE 2. 3D cut of the ELENA source assembly. The main components are highlighted. The beam travels from right to left.

commissioning of all electrostatic transfer lines toward the "old" AD experimental zone. Figure 1 shows a layout of the experimental areas next to the ELENA ring with all transfer lines. The installation is being finalised and the commissioning with H^- is about to start and expected to be completed by mid 2021, when antiprotons will be back in AD and therefore available for experiments.

ELENA ION SOURCE

The ELENA ion source is based on a refurbished and upgraded multi-cusp volume source previously used at the COSY/Jülich injector cyclotron [7], and was originally manufactured by IBA, Belgium. The source, initially foreseen for production of H^- for cyclotrons, can also provide protons by simply reversing the beam potential and the puller voltage. Figure 2 shows an approximate 3D cross-section view of the source assembly as presently installed. Inside the arc discharge chamber a one millimetre diameter electron emitting tungsten filament is heated by a DC current. The filament is biased with respect to the source chamber by a voltage of about 70 V. The arc voltage is static, while the filament heating current is automatically regulated by a feedback such to provide a constant arc current in order to create stable conditions for the ion production. H_2 is injected in from a small orifice at the back of the plasma chamber. For safety reasons and to avoid a complex installation, H_2 is delivered by two Hydrostik cartridges of 10 l each, installed directly next to the plasma chamber. The plasma chamber is surrounded by ten permanent cusp magnets for confinement of the plasma. The magnetic filter, located just in front to the extraction region, is generated by a series of permanent magnets and water-cooled ferromagnetic rods traversing the plasma chamber. The expected magnetic field in the filter region is 260 Gauss. A single electrostatic puller composes the extraction system and the puller electrode is pulsed between negative and positive voltages according to the production of positive or negative ions. The switching is performed by a fast BEHLKE solid state HV switch installed in the Faraday cage. The puller aperture, presently of 4.2 mm diameter, can be exchanged. The puller also hosts permanent magnets deflecting undesired extracted electrons toward the puller itself. A ceramic insulator, only partially shielded [8], insulates the source body from the downstream large chamber at ground potential. A 220 l/s DN200 turbo pump is connected to this chamber. The chamber also hosts an electrostatic quadrupole doublet to allow for optics matching, with steering capability to compensate for unwanted residual deflection by the magnetic filter elements. After the quadrupole doublet, a Pearson Wide Band Current Transformer 5753 [9] is located. This Beam Current Transformer (BCT) is the first instrument able to measure the beam intensity. Recently, the BCT holder has been modified to allow for the addition of either a scintillation screen, or an insulated copper plate with appropriate orifice diameter, acting as a basic Faraday cup and halo collimator.

Typical source parameters are reported in Table I. The puller circuitry was originally designed to minimise the voltage rise time down to about 50 ns as specified in ref. [1]. This was deemed necessary during the ELENA design to ensure beam visibility on the ELENA ring Beam Position Monitors (BPMs) for the first turn, even in case of beam losses on the BPMs electrodes. In practice this was never necessary.

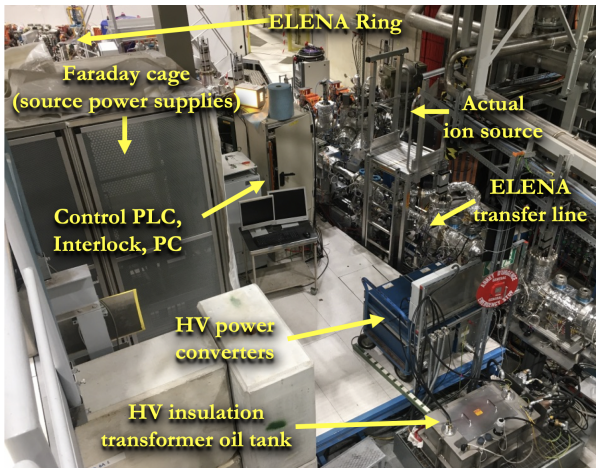

FIGURE 3. Overview of the present source components disposition in the ELENA hall.

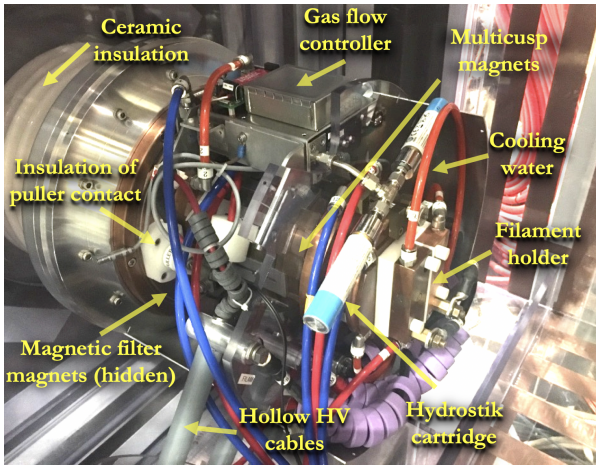

FIGURE 4. View of the source exterior with the HV Corona shield removed with main visible components highlighted.

TABLE I. Main ELENA source parameters and typical operational settings for H^- production.

Parameter	Typical value	Range
Filament diameter	1 mm	-
Filament length	≈13 cm	-
Plasma chamber volume	≈1300 cm^3	-
Filament current	47 A	from 40 A to 53 A
Expected filament temperature	≈2400 K	from 2000 K to 2500 K
Arc voltage	70 V	from 20 V to 80 V
Arc current	2 A	from 1 A to 5 A
Gas injection rate	1 sccm	from 0.6 sccm to 10 sccm
Expected plasma chamber pressure	4×10^{-5} mbar without gas injection	
	1.2×10^{-3} mbar with 1 sccm gas injection	
HV bias	−100 kV	up to ±110 kV
Puller voltages	2650 / − 250 V	up to ±5000 V
Beam pulse length	5 µs	from ≈0.5 µs
Beam pulse rise time	≈100 ns	-
Beam pulse current	≈50 µA	up to ≈150 µA

Due to space constraints, the Faraday cage surrounding the HV cabinet housing the ion source power supplies is separated from the actual ion source with about five meters distance. A general overview of the hardware disposition in the ELENA hall is shown in Figure 3, while Figure 4 shows a picture of the source plasma chamber assembly with the HV Corona shield removed. The original technical drawings of the plasma chamber are available in ref. [10].

OPERATIONAL EXPERIENCE

The main beam characterisation was performed when additional dedicated beam diagnostics was existing [11, 12]. Unfortunately, most diagnostics had to be removed to make room for the installation of the nearby beam transfer lines. The layout of the transfer line that brings the beam to ELENA is shown in Figure 5, which highlights the beam instrumentation presently available to set up and characterise the beam coming from the ion source. The ions coming from the source are bent 43 deg by an electrostatic ion switch. The injection into the ring is achieved with the help of a 340 mrad magnetic septum and an 84 mrad electrostatic kicker whose maximum pulse length is 650 ns with a rise/fall time of circa 200 ns [1]. Typically, a few microseconds-long beam pulse is generated by the ion source and its central part is chopped and injected into the ring by the injection kicker, while head and tail are lost on the ring vacuum chamber. An electrostatic quadrupole doublet and orbit corrector [1] is installed in each straight

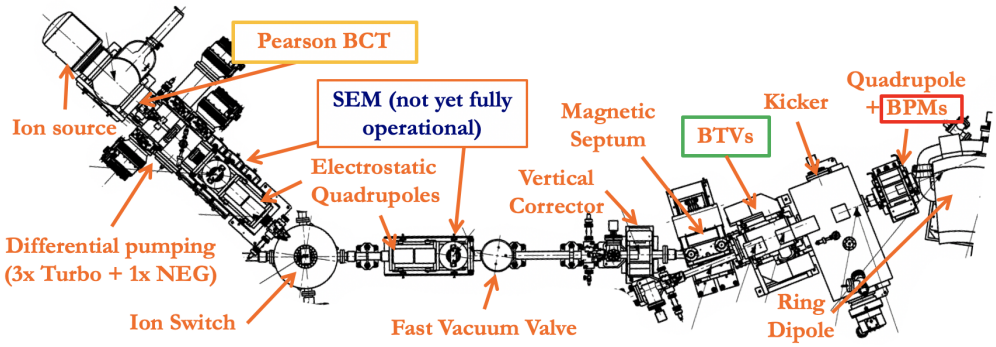

FIGURE 5. Layout of the ELENA injection transfer line from the local ion source and to first part of the ring. The available beam instrumentation is encircled.

section of the injection transfer line. An additional magnetic vertical orbit corrector is installed just before the septum. Two beam profile monitors (SEM) based on photocathode microwire monitors [13] are installed in the transfer line. Unfortunately, those monitors are not yet fully operational due to accumulated delays in the manufacturing of the challenging head electronics and acquisition system and hardware issues with feedthrough connections. Therefore, the first available beam position and profile monitor is a scintillation screen (BTV) installed just after the injection point [14].

Despite the lack of available beam diagnostics, it was possible already in 2016 to inject beam into ELENA [4] with empirical adjustments of the electrostatic and magnetic elements installed along the transfer line. Due to breakdowns in the insulation transformer for the ion source, in 2018 the high voltage bias of the source was reduced to 85 keV. In spite of the lower energy, it was possible to transport the H^- beam to ELENA and quickly accelerate it to 100 keV, or even to the nominal antiproton injection energy of 5.3 MeV, and thereafter decelerate it back to 100 keV [6].

The possibility of having H^- injected in ELENA while awaiting antiprotons has been proven useful, for example for the first setting up and commissioning of the Low Level RF (LLRF) system for the ring [15]. However, since the early stage poor shot-to-shot intensity stability of the circulating beam was observed and required detailed investigation.

Investigation of intra-pulse and shot-to-shot instability

The original BCT installed just after the source [16] was not sufficiently sensitive to record a single shot, and by averaging several shots for noise reduction, the information about intra-pulse instabilities and shot-to-shot fluctuations

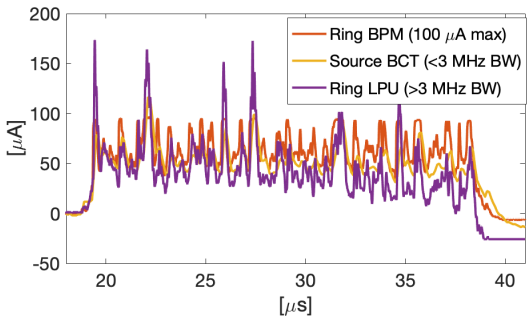

FIGURE 6. Longitudinal beam profile for a single 20 µs-long beam pulse measured with three different beam diagnostic instruments: the BCT installed after the source (yellow), one of the ring BPMs (red) and the ring longitudinal pickup (LPU) (purple).

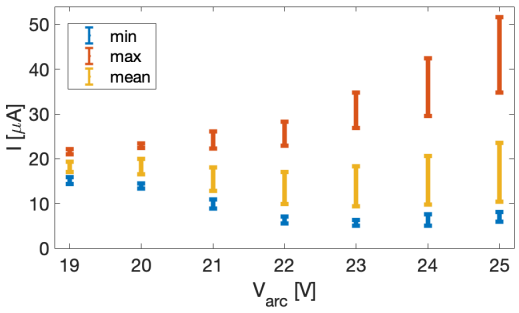

FIGURE 7. Minimum (blue), maximum (red) and mean (yellow) beam current measured over a 10 µs-long beam pulse as a function of arc voltage. The error bar represents the standard deviation over a few hundred shots. The other source parameters were: $V_{puller} = 2650$ V; $I_{filament} = 6\%$, corresponding to $I_{arc} = 1.5$ A; Gas flow 1.7 sccm.

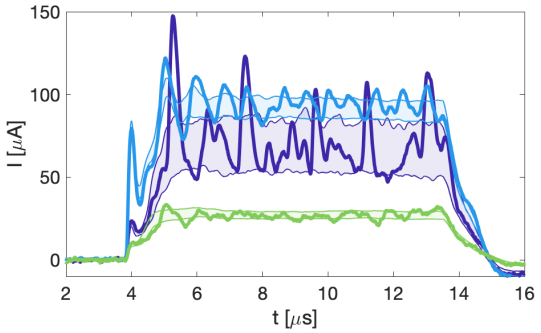

FIGURE 8. H^- intensity along a 10 µs beam pulse measured at the source BCT for different plasma settings. The nominal, unstable, pulse is shown in purple. Operation at lower arc voltage is indicated in green, while operation at higher gas pressure is marked in light blue. The solid line shows a typical pulse, while the shadow area shows the standard deviation over a few hundred pulses.

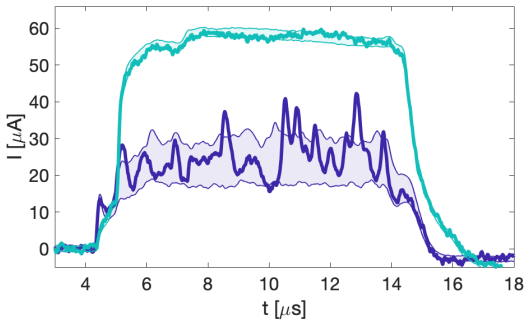

FIGURE 9. Comparison between H^- (turquoise) and positive ion (dark blue) beams with same plasma parameters but inverted puller and HV bias voltages. The solid line shows a typical pulse, while the shadow area shows the standard deviation over a few hundred pulses.

was lost. Only by magnetically injecting the whole beam pulse through the first ring BPM it was possible to reveal an intensity fluctuation along the beam pulse. This instability was thereafter confirmed by using a longitudinal pickup (LPU) installed further down in the ring and it was finally tracked back to the source after installing a more sensitive BCT [9] (x100 more sensitive) together with an ultra low-noise signal amplifier [17] (x800 voltage amplification). The comparison of the observed signals on the different pickups is shown in Fig. 6. Noted that each instrument introduces different signal distortions due to their specifies: the BPM head amplifiers saturates at about 100 µA; the BCT amplifier has a limited bandwidth between ≈1 kHz and ≈1 MHz; while the LPU has slightly higher low- and high-frequency cut offs.

The first attempt to mitigate the instability was to vary the main source parameters: puller voltage, filament current, arc voltage and gas flow. Figure 7 shows the observed beam stability as a function arc voltage while keeping the other parameters constant. For very low arc voltages, the min, max and mean values all tend to about 20 µA, indicating a stable, square pulse. For higher voltages the peak current increases, but the mean current remains low, or even decreases. For higher arc voltages also the minimum beam current is lower than for the minimum arc voltage. When the arc voltage is below 19 V the arc discharge cannot be sustained, and the voltage needs to be raised to approximately 30 V to re-initiate the discharge.

Operating with considerably higher gas flow (about 5 sccm instead of the nominal 1 sccm) also seems to be beneficial for the beam stability. Figure 8 shows a comparison between the following three representative operational scenarios:

- Unstable: Gas flow 1.5 sccm; $V_{arc} = 70\,\text{V}$; $I_{arc} = 2.8\,\text{A}$; $I_{fil} = 46\,\text{A}$
- Low arc voltage: Gas flow 1.5 sccm; $V_{arc} = 23\,\text{V}$; $I_{arc} = 3.5\,\text{A}$; $I_{fil} = 49\,\text{A}$
- High gas flow: Gas flow 5 sccm; $V_{arc} = 70\,\text{V}$; $I_{arc} = 2.8\,\text{A}$; $I_{fil} = 46\,\text{A}$

In all cases the positive puller was set to 2000 V. Please note the remarkably stable pulse for low arc voltage operation, as already seen in Fig. 7, although the beam current is low. On the other hand, for the high gas pressure case the pulse is not as stable, but the current high. For the high gas flow regime, the exceptional stability of the first sub-microsecond peak is of particular interest for injection into the ring.

No characterisation of the beam optics functions and emittance for the different operational scenarios has been attempted yet, but a naive observation of the beam spot seen on the screen in the ring does not show any major difference. So far, no convincing physical explanation for the instability has been found, however, a few observations has been made:

- The typical frequency of the instability is of the order of one MHz, as can be seen for example in Fig. 6.
- The source vacuum chamber was leak tested with no evidence of a leak.

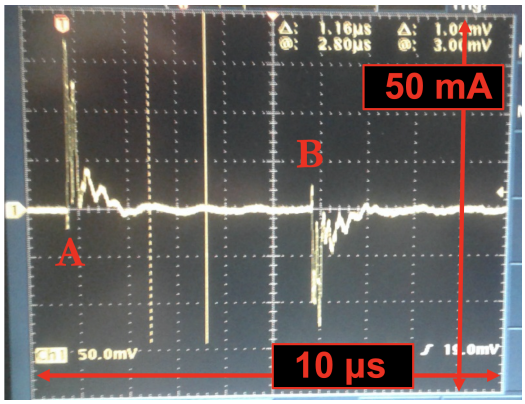

FIGURE 10. Arc current variation as a function of time measured next to the ion source chamber. The highlighted points A and B correspond to the start and end of a 5 µs-long beam pulse.

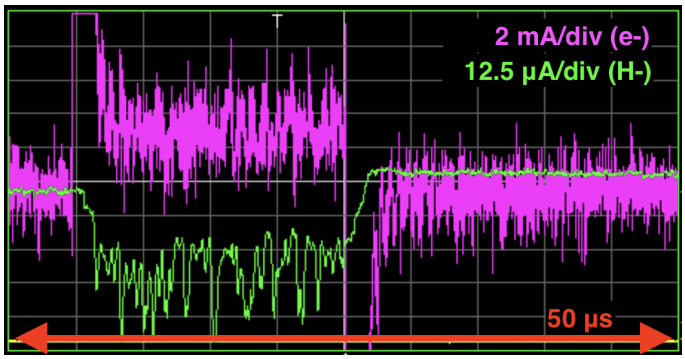

FIGURE 11. Measurement of the e^- current dumped on the puller plate as a function of time (magenta) together with H^- beam intensity (green) measured with the source BCT.

- Figure 10 shows a measurement of the arc current obtained by placing a Pearson 110 current transformer [16] (0.1 Volt/Ampere sensitivity) around the arc return cable about 10 cm from the exit of the plasma chamber. The source was operated with $I_{fil} = 38$ A and $I_{arc} = 1$ A. Such a measurement setup is not responsive to the DC component of the current, but should be sensitive to any current variation within the current transformer bandwidth (1 Hz to 1 MHz). The two peaks correspond to approximately 17 mA current variation, which is significantly lower than the average 1 A arc current, and are related to the switching of the puller electrode in time. No evidence of a typical pattern as seen in Fig. 6 is visible in Fig. 10 neither before, during or after the puller pulse.

- Measurements of electrons dumped on the puller plate have been carried out using a Pearson 4100 current transformer [18] (1 Volt/Ampere sensitivity) with a similar setup as for the arc current. Figure 11 shows a measurement performed with Gas flow 1 sccm; $V_{arc} = 60$ V; $I_{arc} = 3.1$ A; $I_{fil} = 47$ A; $V_{puller} = +920\,\text{V}/-250$ V, but with a HV bias of only 15.6 kV. A high-frequency noise with an amplitude of the order of one mA is always visible on such a measurement and this may mask an instability with the one observed on the H^-.

- One can compute the expected plasma density compatible with a 1 MHz plasma oscillation, neglecting cusp magnetic field, starting from the simple plasma equation: $\omega^2 = \frac{ne^2}{m\varepsilon_0}$, where n is the charge number density, m the particle mass and ε_0 the vacuum permittivity. For electrons this would corresponds to $n_e \approx 1 \times 10^{10}\,\text{m}^{-3}$ and for H^+ to $n_p \approx 2 \times 10^{13}\,\text{m}^{-3}$. Both values seems to be far from the expected H_2 density of $n_{H_2} \approx 3 \times 10^{19}\,\text{m}^{-3}$, corresponding to a vacuum pressure of $\approx 1 \times 10^{-3}$ mbar, thus discarding a pure plasma-oscillation-related instability.

- Figure 9 shows the comparison between H^- and positive ion beam measured with the source BCT by inverting the puller voltage and HV bias voltage while keeping the same plasma parameters: $V_{puller} = \pm 1200$ V; Gas flow 1.5 sccm; $V_{arc} = 70$ V; $I_{arc} = 2.8$ A; $I_{filament} = 46$ A, but for a much lower HV bias of ± 10 kV than nominal. According to the plot the positive ion beam does not exhibit the same instability as observed for the H^-.

All above observations, in particular the results from positive ion extraction, point in the direction of an instability in the H^- production. This is located in the magnetic filter region and therefore not easily visible on most of the external signals available. In the filter region the expected magnetic field generated by the filter magnets is of the order of 260 Gauss. For such a magnetic field, the proton gyrofrequency ($\Omega_{cp} = \frac{eB}{m_p}$) is of the order of 0.4 MHz, which could suggest a relation. On the other hand, the proton gyrofrequency should not be affected by the arc voltage setting and therefore it is not evident how to explain that at low arc voltage the instability seems to disappear, as shown in Fig. 7. Further investigations are therefore needed, eventually supported by detailed simulations taking into account all effects.

High Voltage Insulation Transformer Issues

All devices in the HV cabinet work at 230 V and 400 Hz. The higher frequency was chosen in order to reduce the size of the insulating transformer and in particular to avoid using an oil insulation. Unfortunately, the initially chosen insulating transformer was not able to sustain extended operation at 100 kV. After several attempt with different solid-insulated transformer, it was decided to try with an oil-based one. No off-the-shelf solution was found that met the specifications listed in Table II, and only a few external companies accepted the challenge to produce a transformer working at this higher frequency. The first few versions were only partially successful: during DC operation at 100 kV partial discharges were audible, and, after a few hours of constant operation, they typically sparked between the secondary winding (at high potential) and the magnetic core (as shown in Figure 12) or to the primary circuit, in the latter case damaging the 400 Hz voltage source upstream. The latest insulating transformer version profits of an even larger oil tank and distances between HV and ground components has been increased to respect a maximum peak field of 4 kV/mm. In this transformer version, no audible partial discharges were detected.

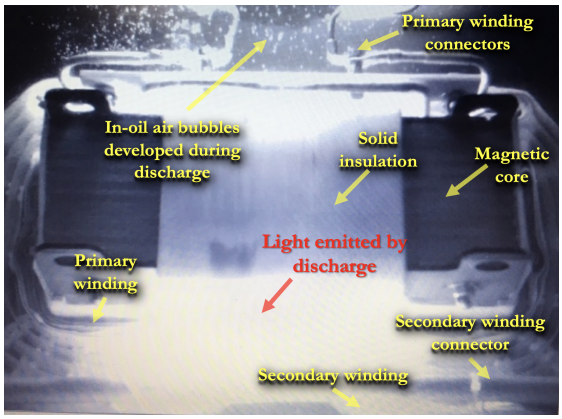

FIGURE 12. Spark between the secondary winding and magnetic core of the insulation transformer in its insulating oil tank caught with a fast camera.

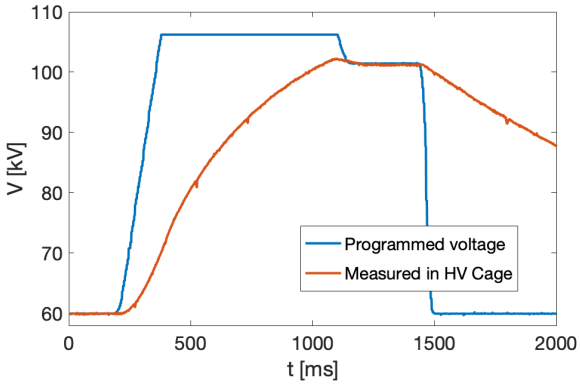

FIGURE 13. Programmed voltage (blue) and measured voltage inside the Faraday cage (orange) as a function of time during pulsed operation of the ELENA source HV.

A possible workaround to the problem has been pulsing of the source HV, which limits the time when the system and so the insulation transformer is at 100 kV potential. Pulsing from 60 kV DC to 100 kV just before beam extraction will reduce the sparking risk significantly, while keeping the ramping time reasonable. In order to achieve pulsed operation it was essential to implement a reliable HV probing of the source potential. This was obtained by converting the Faraday cage 300 MΩ load resistor into a 600 MΩ voltage divider with a 20 kΩ measurement resistor, i.e. with a measurement ratio of 0.033 V/kV. Figure 13 shows the presently pulsing setup. The HV measured in the Faraday cage is much slower than the programmed voltage due to the capacitance of the complete setup and the basic regulation circuit of the HV bias supply, which is not designed for pulsed operation. The requested voltage is higher than 100 kV in Figure 13 in order to partially overcome the regulation circuit deficiencies and slightly speed up the voltage ramp. The 200 ms plateau at 100 kV serve to let stabilise the HV and allow for possible time jitter between the HV pulse and the extracted pulse, which is set to trigger a few milliseconds before the HV is ramped down. In the present setup, the typical HV pulse duration is of the order of 1.5 s, to be compared with a typical repetition period of 4.8 s or more, depending on the ELENA ring magnetic cycle.

Especially challenging was to use positive HV (for proton operation). To date, none of the produced oil-based

TABLE II. Specifications for the ELENA ion source single phase insulation transformer.

Apparent power	$S = 10\,\text{kVA}$
Nominal frequency	$f_n = 400\,\text{Hz}$
Primary nominal voltage	300 V
Secondary nominal voltage	230 V
Insulation from secondary to primary and ground	110 kV DC

transformer was able to sustain 100 kV DC voltage for more than a few minutes. However, the latest insulation transformer version was not tested with positive voltage in order to avoid the risk of damaging it just before the start of the ELENA transfer line commissioning, which is planned to start by end of September 2020. For the same reason, it was decided to keep the HV pulsing option in order to minimise the probability of issues.

OUTLOOK AND CONCLUSIONS

The use of H^- ions for the commissioning of the ELENA ring has been already proven useful, and it will be a necessary tool for the commissioning of the ELENA ring extraction transfer lines.

The long lasting issues with the HV insulation transformer seems to be now under control. The beam produced by the source exhibits some intensity instability. Two workarounds have been identified. At the time of writing, both low-arc-voltage and high-gas-flow regimes seem to be suitable for providing good quality beams to be used for the transfer lines commissioning, with a slight preference for the high gas flow regime that is easier to control and allows to obtain higher beam intensities injected in ELENA, at the expense of having to refill the H_2 Hydrostik cartridges more often, now typically once a week. The actual explanation for the observed instability is still unknown. The most trivial sources of instability have been ruled out. Further analysis would require modifications to the source in order to add dedicated instrumentation, such as photodiodes to study the plasma and the H^- production regions. Other empirical adjustments could be attempted, for example changing the filament shape or the configuration of the permanent magnets used to produce the magnetic filter field.

ACKNOWLEDGMENTS

We wish to acknowledge CERN and Jülich technical services for their continued support towards a reliable and highly performing source for ELENA, in particular Marek Gasior and Francesco Di Lorenzo for their contributions with electronics and signal processing.

REFERENCES

1. C. Alanzeau *et al.*, "Extra Low ENergy Antiproton (ELENA) ring and its Transfer Lines: Design Report," Tech. Rep. CERN-2014-002 (CERN, Geneva, Switzerland, 2014).
2. B. Autin *et al.*, "The antiproton decelerator (AD), a simplified antiproton source (feasibility study)," Tech. Rep. CERN-PS-95-36-AR (CERN, Geneva, Switzerland, 1995).
3. C. Carli *et al.*, "ELENA: Installations and Preparations for Commissioning," in *Proceedings of the 7th International Particle Accelerator Conference, IPAC16* (Busan, Korea, 2016) p. MOPOY009.
4. T. Eriksson *et al.*, "ELENA - From Installation to Commissioning," in *Proceedings of the 8th International Particle Accelerator Conference, IPAC2017* (Copenhagen, Denmark, 2017) p. WEPVA034.
5. G. Tranquille *et al.*, "Commissioning the ELENA Electron Cooler," (2019), presented at the 12th International Workshop COOL2019 in Novosibirsk, Russia, unpublished.
6. D. Gamba *et al.*, "ELENA Commissioning," in *Proceedings of North American Particle Accelerator Conference, NAPAC2019* (Lansing (MI), USA, 2019) p. WEIBB1.
7. R. Gebel *et al.*, "Preparation of an Ion Source for an Extra Low Energy Synchrotron," in *Proceedings of the 6th International Particle Accelerator Conference, IPAC2015* (Newport News (VA), USA, 2015) p. THPF029.
8. The shielding is not visible in Figure 2.
9. P. Electronics, *Pearson Current Monitor 5753*, Palo Alto (CA), USA (), datasheet in `http://www.pearsonelectronics.com`.
10. A. Niaz, ""technical drawings of the elena ion source"," Tech. Rep. CERN EDMS n.1557043 (IBA sa, Louvain-La-Neuve, Belgium, 1991).
11. A. Megía-Macías *et al.*, "The ion source for the commissioning of elena ring," AIP Conference Proceedings **2011**, 090014 (2018).
12. A. Megía, "Elena ion source installation," Tech. Rep. EDMS n.1530395 (CERN, Geneva, Switzerland, 2015).
13. M. Hori, "Photocathode microwire monitor for nondestructive and highly sensitive spatial profile measurements of ultraviolet, x-ray, and charged particle beams," Review of Scientific Instruments **76**, 113303 (2005).
14. G. Tranquille *et al.*, "Commissioning the ELENA Beam Diagnostics Systems at CERN," in *Proceedings of the 9th International Particle Accelerator Conference, IPAC2018* (Vancouver, BC Canada, 2018) p. WEPAF084.
15. M. E. Angoletta *et al.*, "Initial Beam Results of CERN ELENA's Digital Low-Level RF System," in *Proceedings of the 8th International Particle Accelerator Conference, IPAC2017* (Copenhagen, Denmark, 2017) p. THPAB142.
16. P. Electronics, *Pearson Current Monitor 110*, Palo Alto (CA), USA (), datasheet in `http://www.pearsonelectronics.com`.
17. M. Gasior, Private Communication.
18. P. Electronics, *Pearson Current Monitor 4100*, Palo Alto (CA), USA (), datasheet in `http://www.pearsonelectronics.com`.